ASME

An Experimental Study of Upper Hot Layer Stratification in Full-Scale Multiroom Fire Scenarios

L. Y. Cooper

M. Harkleroad

J. Quintiere

W. Rinkinen

National Bureau of Standards, Washingotn, DC

This paper describes an experimental study of the dynamics of smoke filling in realistic, full-scale, multiroom fire scenarios. A major objective of the study was to generate an experimental data base for use in the verification of mathematical fire simulation models. The test space involved 2 or 3 rooms, connected by open doorways. During the course of the study the areas were partitioned to yield four different configurations. One of the rooms was a burn room containing a methane burner which produced either a constant energy release rate of 25, 100, or 225 kW or a time-varying energy release rate which increased linearly with time from zero at ignition to 300 kW in 10 min. An artificial smoke source near the ceiling of the burn room provided a means for visualizing the descent of the hot layer and the dynamics of the smoke filling process in the various spaces. The development of the hot stratified layers in the various spaces was monitored by vertical arrays of thermocouples and photometers. A layer interface was identified and its position as a function of time was determined. An analysis and discussion of these results are presented.

NOMENCLATURE

A_B, A_C, A_L	areas of burn room, corridor, and lobby
C_p	specific heat at constant pressure
e	specific internal energy
H	floor-to-ceiling height
h, h_{amb}	specific enthalpy and its ambient value
N	value of N in N percent rule, Eq. (2)
n	an integer
$\bar{n}$	unit normal vector
P	absolute pressure
Q	total energy release rate of fire
Q_{ramp}	value of Q for ramp fire, Eq. (1)
S	internal bounding surface of enclosure
T, T_{amb}	temperature and its ambient value
t, t*	time after ignition
$\bar{V}$	velocity vector
z	distance above floor
z_i	z for interface
z_{top}	z for top thermocouple or photometer
Δp	burn room-corridor ceiling pressure difference
$\overline{\Delta T}_A$, $\overline{\Delta T}_D$, $\overline{\Delta T}_E$	$\overline{\Delta T}$ at positions A, D, and E
ΔT_{min}	a minimum value of $N\Delta T_{ref}/1000$
ΔT_{ref}	a reference temperature difference, see above Eq. (2)
$\overline{\Delta T}$	vertical average of $T-T_{amb}$
Δz_n	vertical distance associated with thermocouple n
λ_r	fraction of Q radiated from fire
λ_c	fraction of Q transferred out of S
ρ, ρ_{amb}	density and its ambient value
τ	volume of enclosure

INTRODUCTION

In recent years there has been considerable research activity in the dynamic modeling of environmental conditions which develop in enclosed spaces as a result of hazardous fires. Attention was originally focused on single space enclosures with ventilation from single openings [1,2,3] (a closed or partially opened window or door). Work has recently been initiated on the development of computer programs which model the spread of combustion products through connected, multiroom configurations with multiple ventilation openings [4,5,6]. In order to gain confidence in these analytic tools, and to improve their predictive capability, comparisons between theory and full scale experiments are required. To some extent such comparisons have already been successfully carried out [7,8,3].

Contributed by the Heat Transfer Division of THE AMERICAN SOCIETY OF MECHANICAL ENGINEERS for presentation at the 20th Joint ASME/AIChE National Heat Transfer Conference, Milwaukee, Wisconsin, August 2-5, 1981. Manuscript received at ASME Headquarters April 14, 1981.

Copies will be available until May 1, 1982.

A major goal of all this mathematical modeling activity is to provide a tool for estimating the development of hazardous conditions in real fire scenarios. In terms of life safety considerations, one is particularly concerned with reasonably accurate modeling of the environmental conditions from the time of fire ignitions until the time when life threatening conditions start to prevail. It is during such time intervals that successful fire detection and occupant egress must occur if a basic condition of safety is to prevail in an occupancy of interest [9]. The present experimental study is concerned with these relatively early time intervals which immediately follow the ignition of life threatening fires.

OBJECTIVE OF THE STUDY

Enclosure fire models differ in a variety of ways. An example of where considerable variation exists is in the degree of detail in the physical description of the actual combustion zone located in the room of fire origin. In spite of such differences there is one feature which is common to all single or multiroom zone-type enclosure fire models; namely, a two-layer description of the intraroom environmental conditions. In the two-layer description, the environment in each room of a modeled space is described by a uniform lower layer of relatively cool and unpolluted ambient air and by a uniform upper layer of elevated temperature, and partially diluted products of combustion. The two layers are assumed to be divided by a sharp horizontal material interface. In the room of fire origin, the products of combustion are diluted with entrained lower layer ambient air as they rise in a plume from the combustion zone itself to the developing upper layer. In the vicinity of open connecting doorways or windows, the upper layer and lower layer of the burn room exchange mass with the layer pairs of adjacent spaces. Similar continuous exchanges between all other connected adjacent spaces also takes place as the various upper layers continue to grow in depth, in temperature and in combustion product concentration.

If the simulations of a specific mathematical model (which incorporates the two layer approach) are to be used with confidence for a given class of threatening fire scenario, then at least two prior conditions must have been met. The first condition is that the two-layer model is shown to represent a reasonable qualitative description of the real fire environments of interest. The second condition is that quantitative predictions of the model compare favorably with actual data acquired during full scale fire tests. Furthermore, these latter prototype fire tests should cover a significant range of the key parameters which are descriptive of the class of threatening fire scenario of interest.

It was the objective of the present study to generate an experimental data base on the dynamics of smoke filling in realistic full scale multiroom fire scenarios so that the data generated by these tests, and tabulated here will provide a basis for the above mentioned comparative checks between theory and experiment.

DESCRIPTION OF THE TEST PROGRAM

The test program consisted of a series of separate tests involving a variety of space configurations and fire energy release rates.

For a given test the test space involved either 2 or 3 rooms connected by open doorways, all having a nominal 2.36 m ceiling height. The wall and ceiling surfaces of all rooms were lined with 13 mm thick gypsum board, and the floors were concrete. During the course of the test program the space was partitioned to yield four different configurations ranging in total plan area from 40.6 m^2 to 89.6 m^2. These configurations are sketched in Figure 1. The doorway between the burn room and its adjacent space (designated here as the corridor) was 2.0 m high and 1.07 m wide. The doorway between the corridor and the next adjacent space (designated as the lobby) was 2.01 m high and 1.32 m wide.

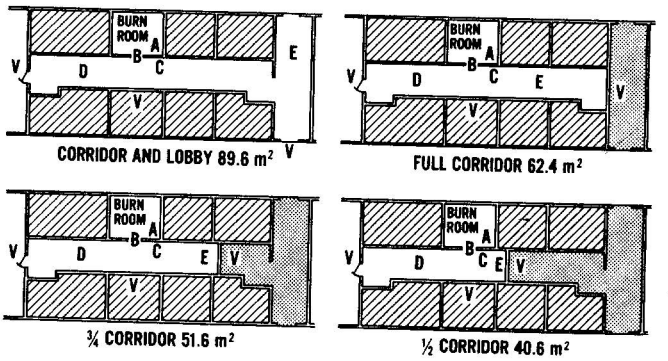

Fig. 1 Sketches of four test configurations with indications of the location of vertical instrument arrays (A,B,C,D, and E) and of video cameras (V).

An attempt was made to seal cracks and penetrations in the bounding surfaces of the test space. A 0.15 m x 0.94 m hole with clear opening to the outside (through an unused room and open window of the test facility) was provided next to the floor in a wall surface of the corridor. In concert with the above attempts at sealing all surfaces, the hole was to provide the major leakage path for mass exchanges between the test space and the outside environment.

Each test used the same burn room of 14.0 m^2 area. The room contained a 0.30 m x 0.30 m square methane diffusion burner whose burn surface was positioned 0.24 m above the floor and approximately in the center of the room. After ignition from a pilot light, fuel supply to the burner was manually controlled from an outside metering system to produce one of four possible energy release rates; a constant rate, Q, of 25 kW, 100 kW or 224 kW or a time varying energy release rate, $Q_{ramp}(t)$, of

$$Q_{ramp}(t) = 30\ t\ kW, \quad 0 \leq t\ (t \text{ in minutes}) \qquad (1)$$

where the time from ignition, t, never exceeded 10 minutes. These bear a similarity to energy rates that would develop from fires in wastepaper baskets, upholstered chairs and mattresses.

McCaffrey [10] has studied the free burn characteristics of the particular burner used in these tests. Using methane for a fuel, and for fire powers between 50 kW and several hundreds of kW he found that, of the total energy release rate of the fire, a fraction, λ_r, of approximately 0.24 is radiated away from the combustion zone. For a 25 kW fire power he found λ_r to be 19 percent.

With methane as a fuel the burner produced very little smoke. In order to have a visual tracer of the combustion products as they spread throughout the space, an artificial source of smoke was introduced into the ceiling jet of the burn room. Thus, in every test a highly visible white smoke was generated by a smoke candle and mixed with the fire's products of combustion near their source for up to five minutes. Effective visualization of the upper smoke layers was achieved by deploying flourescent light fixtures on the floor of the corridor and lobby.

For each of the four spatial configurations of Figure 1, a separate burn test was run for each of the four energy release rates (16 test runs). For the 100 kW fire power and full corridor configuration of Figure 1, three additional tests were also run. In these test runs the burn room-to-corridor doorway width was reduced to 1/2, 1/4, and 1/8 of its full value.

INSTRUMENTATION

The data acquired during the tests included temperature measurements from vertical arrays of eight thermocouples each. The arrays were located at positions A, B, C, D, and E which are identified in Figure 1. Note that the position of E shifts from one configuration to the next, but that positions A, B, C, and D are identical for all configurations. Bare wire, 0.25 mm Chromel-Alumel thermocouples were used. Except for doorway position, B, all arrays used identical 0.30 m spacing of the thermocouples with the bottom one being 0.15 m from the floor and the top one being approximately 0.07 m from the ceiling. For the B array the top and bottom thermocouples were 0.30 m, respectively, from the doorway lintel and the floor, and the spacing of all thermocouples was approximately 0.20 m.

Visual evidence of the development and growth of combustion product laden upper layers was obtained by vertical arrays of photometer transmitter-receiver pairs, each transmitter and receiver being separated by a horizontal distance of 1 m. The photometers had been used previously by Bukowski and are described in [11]. The arrays each had four photometer pairs, and they were located at positions B, D, and E. The photometers at B were positioned 1.04 m, 1.38 m, 1.73 m and 1.91 m above the floor, while those at D and E were positioned 0.33 m, 0.93 m, 1.56 m and 2.19 m above the floor. (In the corridor-lobby configuration the 0.33 m photometer was not deployed.)

Visual evidence of layering was also obtained by post-test observations of video tapes which recorded the obscuration of vertical arrays of miniature incandescent lights. Two arrays of lights were set up at positions D and E. The lights were placed adjacent to and at identical elevations of the D and E thermocouple arrays.

A separate video tape recorder camera with lens approximately 0.5 m from the floor was directed at each of the two arrays of lights. A third video recorder camera was placed directly across the corridor from the burn room with full view of the

burner surface, the pilot and the near-ceiling smoke candle. The three cameras were positioned immediately outside of the test space at locations indicated in Figure 1. Visual access for the first two of these cameras was through plastic inserts in closed doors at the ends of the corridor, or, in the case of the corridor-lobby configuration, at the end of the lobby and at the closed end of the corridor. The third camera viewed the burn room through a plastic insert in the corridor wall.

A single pair of static pressure taps, located at positions A and C and approximately 0.05 m from the ceiling was used to measure the pressure difference between the burn room and the corridor. The measuring system had been used previously by Steckler, and it is described in [12]. With the A and C thermocouple array data and this reference pressure difference it should be possible to construct the time varying vertical pressure difference field that drives the flow across the burn room-corridor doorway.

During every test a multichannel analog-digital recorder system acquired the data from all the thermocouples and photometers and from the single pressure difference transducer at five second intervals.

EXPERIMENTAL PROCEDURE

The procedure during a given test run was as follows:

All photometer lenses were cleaned and their outputs were nulled. A member of the test team lit the pilot and evacuated the test space. The smoke candle fuse was ignited by means of wooden matches which were themselves ignited with an externally activated electrically controlled hot wire. At the instant that the candle started to smoke, as viewed from the cross-corridor camera, the fuel control system was operated to provide the appropriate rate of fuel supply, and the data acquisition recorder was activated.

The conditions in the test space were observed by television monitors which received the signals from the three video cameras. The test continued for 1-3 minutes past the time that smoke obscured the entire test space. At this time the fuel supply, the pilot, and all data collection was terminated. The doors to the test space were opened, and a forced ventilation system was used to clear the smoke.

The tests were run during the daytime in the summer. Tests were separated by a time interval of at least two hours so that at the beginning of a run the test space would be smoke-free and with ambient temperature surfaces.

RESULTS AND DISCUSSION

General Observations

In terms of visual observations, a two-layer description of the environments was well substantiated throughout each room, for all test cases, and at least until the upper smoky layer thickness increased to 1/2-2/3 of the total floor-to-ceiling height. After that, the interface position became significantly more diffuse, and the optical density of the corridor (and lobby) lower layers appeared to steadily increase to a state of total obscuration.

The two-layer visualization remained sharper to greater interface depths for tests with more rapid growth of upper layer thickness, (i.e., for test runs with relatively larger fires and relatively smaller floor areas).

Even at early times, though much more so at later times, the introduction of smoke from the upper layer to the lower layer was observed to be by descending wall jets or (inverted) thermals. It is conjectured that these wall layers were generated in the elevated temperature upper layer as a result of heat transfer from the near-wall gases to the relatively cool wall surfaces. Surface cooling of these gases would result in downward directed low speed wall jets (net buoyant forces near the wall being directed downward toward the floor). These would emerge from the upper layer and continue their descent into the lower layer. Once in the cool lower layer, reverse net buoyant forces on these warm wall jets would retard their descent and promote their mixing with the relatively cool and clear lower layer environment.

Position of the Interface

A major purpose of the test program was to generate a data base that would be generally available for future comparisons with the predictions of analytic models. A useful component of such a data base would be the interface elevation in each separate space for a given test run. It is possible to construct such elevation histories from the thermo-

couple data, the photometer data, and the light obscuration data. However, to do this, an operational definition of the precise position of the interface is required. Thus, although the above-mentioned qualitative visual observations are consistent with a two (homogeneous) layer sharp interface type of zonal model, this is not necessarily the case of the quantitative data of, say, the vertical thermocouple arrays.

An example of the rather diffuse nature of the interface as viewed from the perspective of the thermocouple data is indicated in Figure 2. There, the thermocouple data from the corridor arrays C, D, and E are plotted at time t = 165 sec when the visual observations of light array obscuration at both positions D and E indicated (to within five seconds) an interface position 0.76 m above the floor. It is evident from this plot that a two-homogeneous-layer description of the environment in the corridor is an approximation to the actual state. In order to use such an approximation an interface position must be determined from an unambiguous, albeit subjectively formulated, temperature and photometer data reduction scheme. Toward this end the following N percent rule for defining interface elevation was formulated:

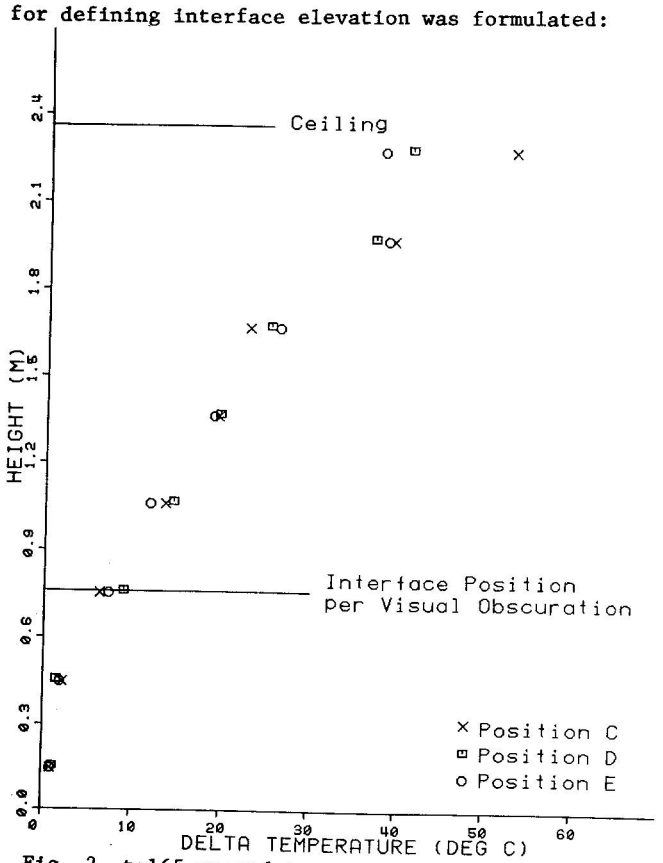

Fig. 2 t=165 second temperatures at corridor positions, C,D, and E; 100 kW, full corridor.

First the rule to be used with thermocouple arrays: At a specific time into a test run one computes a reference upper layer temperature difference $\Delta T_{ref}(t) = \max [T(z_{top}, t)] - T_{amb}(z_{top})$ where $T(z,t)$ is the temperature at elevation z and time t, z_{top} is the elevation of the top thermocouple, $T_{amb}(z) = T(z, t = 0)$ and $\max [T(z,t^*)]$ is the maximum value of $T(z,t)$ in the time interval $0 \leq t \leq t^*$. Then by the N percent rule the interface is defined as passing the elevation $z_i(t)$ at that time t when z_i first satisfies.

$$T(z_i,t) - T_{amb}(z_i) = N\Delta T_{ref}(t)/100 \qquad (2)$$

Also, z_i is defined as monotonic in t, i.e., as time goes on it is assumed that the upper layer never decreases in thickness. Finally, to account for experimental error in temperature measurements it is reasonable to apply the rule only at such times when the right hand side of Eq. (2) exceeds some minimum value ΔT_{min}. (ΔT_{min} here was taken to be 0.5°C.)

An analogous N percent rule to be used with vertical photometer arrays was also formulated, by interpreting z_{top} as the elevation of the top photometer, and by appropriately substituting optical density for temperature in the above. An interface definition similar to the N percent rule was used in [8].

Results of applying the above rule for N = 10, 15, and 20 were obtained for all thermocouple and photometer array data of the 100 kW, full corridor test run (intermediate fire size, intermediate area). The reduced data points for interface elevation which correspond to the fire array locations A-E are plotted in Figures 3a-e, respectively. The 10, 15, and 20 percent rule was also applied to the D array data acquired during the 25 kW, corridor-lobby test run (smallest fire, largest space) and during the 225 kW, 1/2 corridor test run (largest fire, smallest space). These latter results are plotted in Figures 3f and g. Also included in Figures 3d-g are interface elevation data points obtained from the time of obscuration of the vertical light arrays at D and E. These data were generated by one number of the test team who reviewed the appropriate video tape data. Finally, each of the Figures 3a-g includes an analytic estimate of the history of the interface elevation. These curves, designated as single room estimates, are predictions of the interface histories that would

result from point sources of strength $(1-\lambda_r)Q$ located on the floors of single room enclosures (with leakage from below) whose areas are identical to the total plan areas of the respective multiroom spaces [1,9]. It has been suggested in [9] that for "freely connected" multiroom enclosure fires such relatively easily obtainable predictions may provide reasonable approximations to actual interface elevation histories. The present experiments appear to provide a degree of support for this contention.

From a study of the data of Figure 3 it was concluded that application of the 10 percent rule would provide a reasonable basis for an experimentally determined interface elevation history. The rule for N = 10 was therefore applied to all data of all test runs. The results are presented in Table 1. Also included in Table 1 are the interface elevation histories determined from observations of vertical light array obscuration.

Vertically Averaged Temperatures

It is beyond the intended scope of the present paper to include all of the thermocouple data acquired during the test program. Nevertheless, results which indicate the actual magnitude of the measured temperature increases (as compared to the relative distribution of temperatures per Table 1) would constitute a valuable addition to the data base presented here. Toward this end and for the neighborhood of any particular thermocouple array the time-varying vertically averaged temperature increase, $\overline{\Delta T}$ is estimated from

$$\overline{\Delta T}(t) = \frac{1}{H}\int_0^H [T(z,t)-T_{amb}(z)]dz$$

$$\approx \frac{1}{H}\sum_{n=1}^{8} [T(z_n,t)-T_{amb}(z_n)]\Delta z_n \qquad (3)$$

where z_n corresponds to the elevation of the nth thermocouple in the array, and Δz_n is the vertical zone of influence associated with this thermocouple. Eq. (3) was applied to all arrays but B. In doing so, Δz_1 to Δz_7 were taken to be .305 m, and Δz_8 was taken to be between .191 and .241 m depending on location.

As an illustration of the above data reduction scheme the $\overline{\Delta T}$'s from the thermocouple arrays of the 100 kW full corridor test and the full corridor ramp fire test are plotted in Figures 4a and b, respectively. The scheme was carried out for all test runs, and smoothed results are presented in Table 2 for arrays

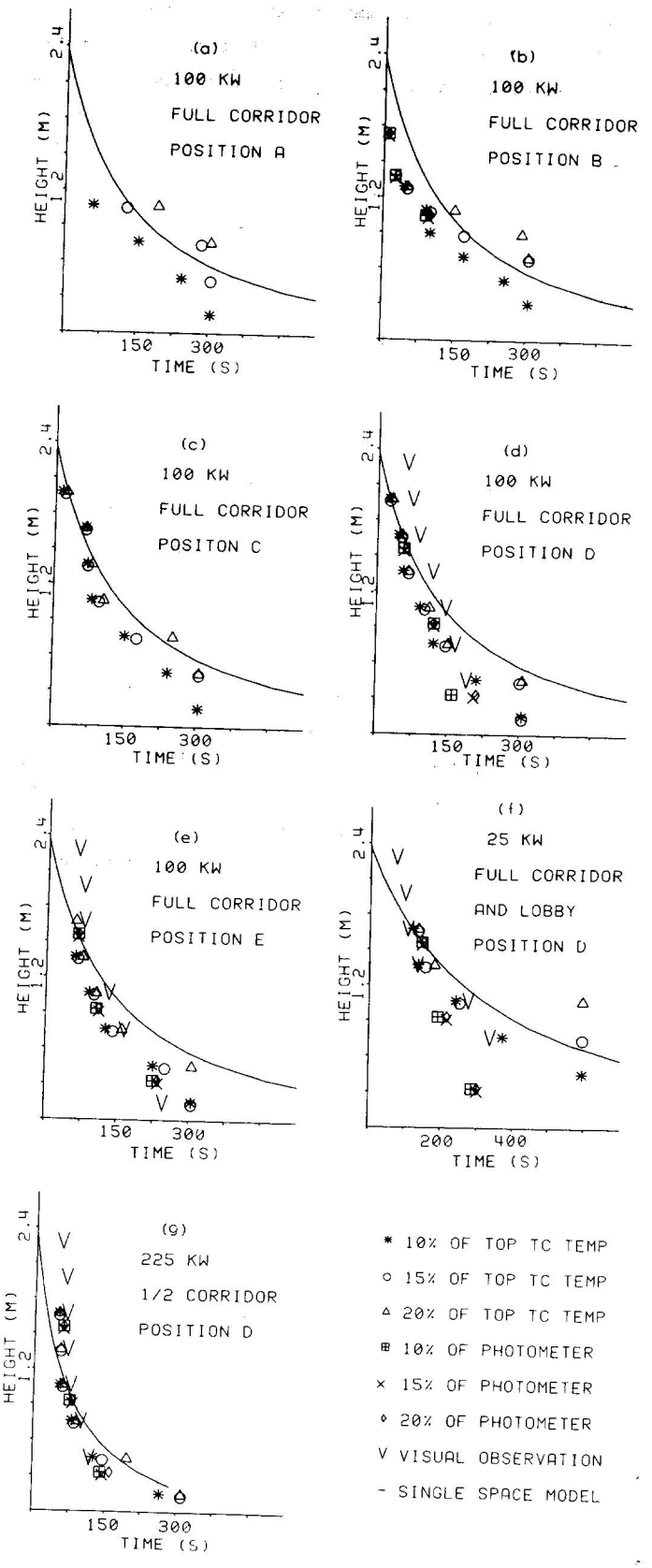

Fig. 3 Elevation of interface according to 1) N percent rule for N=10, 15, and 20 as applied to thermocouple data and photometer data, 2) obscuration of light array, and 3) single room model.

A and D, and, in test runs with corridor-lobby configurations, for array E.

In Figures 4a and b the similarity between the $\overline{\Delta T}$ histories associated with all corridor thermocouple arrays is noteworthy. A study of all corridor array $\overline{\Delta T}$'s revealed the persistance of this result during all test runs. This is an indication of the relative uniformity in conditions along the length of the corridor. On account of this uniformity, only $\overline{\Delta T}_D$ of the corridor arrays is included in Table 2.

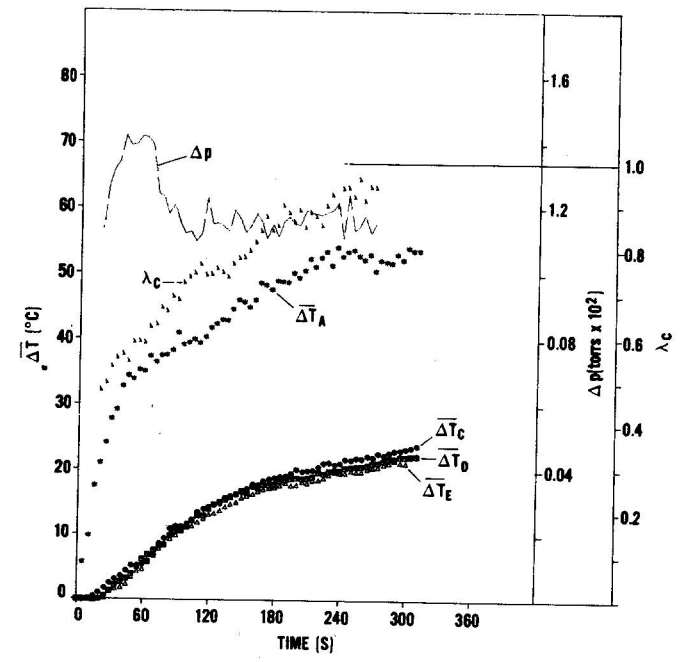

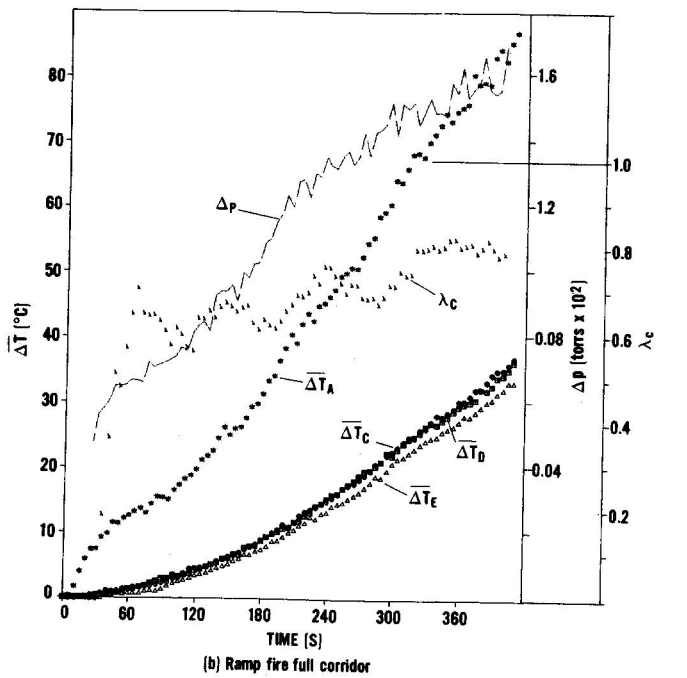

Fig. 4 Vertically averaged temperature changes per Eq. (3) at burn room and at corridor arrays; λ_c per Eq. (4); pressure difference, Δp, across doorway.

The Heat Transfer to Bounding Surfaces

A necessary prerequisite to the successful modeling of enclosure gas temperatures is an estimate of the total rate of heat transfer to bounding surfaces of the enclosure. As indicated in [9] it is useful to express this heat transfer as a fraction, λ_c, of the fire's instantaneous energy release rate. Thus, $\lambda_c Q(t)$ is defined as the instantaneous total rate of heat transfer, radiation plus convection, to the bounding surfaces of the enclosure.

According to a derivation presented in the Appendix, λ_c in the present experiments can be estimated from

$$\lambda_c(t) = 1 - \frac{\rho_{amb} C_p \tau}{Q(t)} \frac{d\overline{\Delta T}(t)}{dt} \qquad (4)$$

where ρ_{amb} is the ambient density, C_p is the specific heat at constant pressure and τ is the total volume of the test space. Here $\overline{\Delta T}$ is the temperature increase above ambient averaged over the entire test space, and it can be estimated from

$$\overline{\Delta T}(t) = \frac{A_B \overline{\Delta T}_A(t) + A_C \overline{\Delta T}_D(t) + A_L \overline{\Delta T}_E(t)}{A_B + A_C + A_L} \qquad (5)$$

where A_B is the area of the burn room, and A_C and A_L are the utilized areas of the corridor and lobby, respectively. With the results of the previous section and using data smoothing techniques $\lambda_c(t)$ has been obtained from Eqs. (4) and (5) for all test runs. These λ_c histories are presented in Table 2. The values of ρ_{amb} and C_p were taken as 1.18 kg/m^3 and 240 cal/kg°C), respectively. λ_c is plotted in Figures 4a and b for the 100 kW, full corridor test and for the full corridor, ramp fire test, respectively.

It should be noted that the Table 2 estimates of λ_c do not account for the changing enthalpy content of the plume and ceiling jet. This could lead to large errors at early times of a test run when a significant fraction of the $d\overline{\Delta T}/dt$ of Eq. (4) is associated with the gases in these zones. At t = 60 sec, when such errors in the λ_c estimates are likely to be less important, the heat transfer losses for all test runs are in the range of 51-74 percent of Q. At this time heat transfer is still mainly to the

Table 1. Time in seconds after ignition when the layer passes a given z elevation according to:
T_D - vertical thermocouple array at position D per 10 percent rule;
P_D - vertical photometer array at position D per 10 percent rule;
V_D - visual obscuration of vertical light array at position D;
etc.

Z meter	T_A	T_C	T_D	P_D (V_D)	T_E	P_E (V_E)	Z meter	T_B	P_B
25 kW 1/2 corridor									
2.29				(81)		(63)			
1.98				(97)		(102)	1.73		5
1.68			70	(110)		(115)	1.49		
1.56				85			1.38		45
1.37		35	75	(117)	105	(173)	1.29	85	
1.07	110	120	80	(139)	115	(183)	1.09	115	
.93				130			1.04		110
.76	185		140	(186)	130	(195)	.90	145	
.46	190	130	280	(200)		(217)	.70	165	
.33				250			.50	255	
.15	425	425	425		425		.30	410	
25 kW full corridor									
2.29				(81)		(69)			
1.98		55		(101)		(113)	1.73		15
1.68	20	125	100	(105)		(118)	1.49		
1.56				105		125	1.38		55
1.37		140	110	(144)	120	(131)	1.29	80	
1.07	50	150	165	(215)	155	(185)	1.09	170	
.93				210		170	1.04		135
.76	175	255	220	(241)	165	(211)	.90	205	
.46	245	320	310	(278)	175	(264)	.70	295	
.33				230		270	.50	410	
.15	590	610	595		555	(233)	.30	610	
100 kW 1/2 corridor									
2.29				(47)					
1.98		15		(57)	10		1.73		10
1.68	50		40	(62)			1.49		
1.56				50			1.38		30
1.37		55		(68)	55		1.29		
1.07		65	50	(77)	65		1.09	60	
.93				75			1.04		65
.76	95	70	75	(94)	75		.90	80	
.46	140	125	135				.70	90	
.33				145	125		.50	125	
.15	280	295	250		295		.30	295	
100 kW full corridor									
2.29				(61)		(63)			
1.98		15	25	(72)		(76)	1.73		10
1.68		65	45	(87)		(77)	1.49		
1.56				55		65	1.38		25
1.37		70	55	(116)	60		1.29	45	
1.07	60	80	90	(144)	90	(131)	1.09	90	
.93				120		105	1.04		90
.76	155	150	120	(165)	125	(164)	.90	100	
.46	245	240	210	(189)	225		.70	170	
.33				160		225	.50	255	
.15	305	305	305		305	(246)	.30	305	
225 kW 1/2 corridor									
2.29				(54)					
1.98		20		(64)	20		1.73		20
1.68			45	(67)			1.49		
1.56				60			1.38		25
1.37		55		(70)	55		1.29		
1.07		65	50	(77)	60		1.09		
.93				75			1.04		70
.76	100	70	75	(99)	70		.90	75	
.46	120	120	120	(117)	130		.70	85	
.33				140			.50	110	
.15	235	305	260		305		.30	245	
225 kW full corridor									
2.29				(55)		(60)			
1.98		15		(70)		(66)	1.73		10
1.68		50	35	(79)	45	(70)	1.49		
1.56				45		65	1.38		35
1.37		55	45	(99)		(85)	1.29	45	
1.07		65	85	(110)	70	(107)	1.09	80	
.93				95		100	1.04		70
.76	135	130	105	(127)	100	(135)	.90	100	
.46	190	190	200	(138)	185	(158)	.70	160	
.33				175		195	.50	205	
.15	305	305	305		305		.30	305	
ramp fire 1/2 corridor									
2.29				(88)		(78)			
1.98				(100)		(87)	1.73		25
1.68	85		90	(103)		(109)	1.49		
1.56				95			1.38		60
1.37		105		(109)	110	(147)	1.29	80	
1.07		120		(126)	125	(164)	1.09	110	
.93				115			1.04		120
.76	150	130		(145)	130	(168)	.90	120	
.46	165	135	210	(166)	140		.70	160	
.33				195			.50		
.15	305	305	305		305		.30	305	
ramp fire full corridor									
2.29				(70)		(80)			
1.98		30		(85)		(89)	1.73		5
1.68		100	70	(109)		(96)	1.49		
1.56				75		95	1.38		75
1.37		110		(129)	90	(129)	1.29		
1.07	30	140	130	(167)	125	(155)	1.09	145	
.93				165		150	1.04		115
.76	210	185	185	(192)	185	(200)	.90	155	
.46	300	300	280	(222)	295	(243)	.70	275	
.33				190		230	.50	305	
.15	305	305	305		305	(243)	.30		

Z meter	T_A	T_C	T_D	P_D (V_D)	T_E	P_E (V_E)	Z meter	T_B	P_B
25 kW 3/4 corridor									
2.29				(68)		(86)			
1.98		25		(86)		(99)	1.73		15
1.68		65	65	(99)		(107)	1.49		
1.56				35		60	1.38		65
1.37		70	70	(106)		(152)	1.29		
1.07		120	100	(136)		(183)	1.09	115	
.93				115		155	1.04		105
.76			150	(187)	150	(263)	.90	145	
.46	290	245	215	(221)	175	(317)	.70	195	
.33				120		250	.50	270	
.15	370	370	370		365	(266)	.30	370	
25 kW full corridor and lobby									
2.29				(72)		(124)			
1.98				(97)		(162)	1.73		60
1.68			120	(105)			1.49		
1.56				145		270	1.38		105
1.37			135	(133)		(227)	1.29		
1.07	105		240	(274)		(243)	1.09		
.93				190		275	1.04		145
.76	210		370	(335)		(281)	.90	315	
.46	595	430	595			(265)	.70	595	
.33				285		280	.50		
.15		595			590		.30		
100 kW 3/4 corridor									
2.29				(48)		(60)			
1.98		20		(59)		(65)	1.73		0
1.68		45	45	(67)		(111)	1.49		
1.56				55		35	1.38		15
1.37		50	50	(71)	35	(120)	1.29		
1.07		85	70	(98)	90	(149)	1.09	75	
.93				85		105	1.04		70
.76	90	110	100	(126)	105	(209)	.90	80	
.46	125	170	180		125	(181)	.70	135	
.33				175		140	.50	210	
.15	360	360	360		360		.30	360	
100 kW full corridor and lobby									
2.29				(107)		(64)			
1.98				(120)		(74)	1.73		
1.68		135	115	(160)	155	(88)	1.49		
1.56							1.38		
1.37		145	120	(175)	170	(119)	1.29		
1.07		155	260	(187)	205	(261)	1.09		
.93							1.04		
.76		435	360	(214)		(311)	.90	410	
.46	435		435	435	305		.70	435	
.33							.50		
.15					435		.30		
225 kW 3/4 corridor and lobby									
2.29				(52)		(85)			
1.98		20		(60)		(84)	1.73		0
1.68		40	40	(66)	30	(115)	1.49		
1.56				50		35	1.38		5
1.37		55	50	(77)		(144)	1.29	35	
1.07	65	65	55	(88)	70	(152)	1.09	60	
.93				70			1.04		65
.76	75	90	85	(112)	90	(177)	.90	75	
.46	155	155	155	(152)	120	(179)	.70	105	
.33				150			.50	155	
.15	295	335	340		330		.30	310	
225 kW full corridor and lobby									
2.29						(82)			
1.98		15		(121)		(93)	1.73		15
1.68		50	35	(123)	70	(114)	1.49		
1.56				190		60	1.38		40
1.37		60	45	(137)	100	(161)	1.29		
1.07		160	150	(149)		(224)	1.09		
.93				195		95	1.04		120
.76	230	340	235	(177)	140	(242)	.90	205	
.46	295	365	365	(234)	215	(283)	.70	365	
.33				200		100	.50		
.15	365			(257)	365		.30		
ramp fire 3/4 corridor									
2.29				(92)					
1.98				(113)			1.73		120
1.68		105	110	(123)			1.49		
1.56				120		100	1.38		65
1.37		145	115	(129)			1.29	70	
1.07	125	180	145	(141)			1.09	165	
.93				150		155	1.04		130
.76	225	190	170	(178)	195		.90		
.46	315	265	245		225		.70	250	
.33				225		225	.50	265	
.15	360	360		360			.30	345	
ramp fire full corridor and lobby									
2.29				(96)		(130)			
1.98				(108)		(184)	1.73		120
1.68		250	190	(120)	280	(210)	1.49		
1.56				220		335	1.38		170
1.37	130	280		(171)	310	(221)	1.29		
1.07	145	335	315	(298)	325	(227)	1.09	335	
.93				340		340	1.04		260
.76	475	690	595	(360)	340	(261)	.90	510	
.46	590	720	720		475		.70	720	
.33				350		345	.50		
.15	720				720	(281)	.30		

Table 1. Continued

ramp fire full corridor									
Z meter	T_A	T_C	T_D	P_D (V_D)	T_E	P_E (V_E)	Z meter	T_B	P_B
2.29				(70)		(80)			
1.98		30		(85)		(89)	1.73		5
1.68		100	70	(109)		(96)	1.49		
1.56				75		95	1.38		75
1.37		110		(129)	90	(129)	1.29		
1.07	30	140	130	(167)	125	(155)	1.09	145	
.93				165		150	1.04		115
.76	210	185	185	(192)	185	(200)	.90	155	
.46	300	300	280	(222)	295	(243)	.70	275	
.33				190		230	.50	305	
.15	305	305	305		305	(243)	.30		
100 kW full corridor 1/2 door									
2.29				(75)		(77)			
1.98		25	40	(97)		(94)	1.73		10
1.68		75	60	(118)	65	(96)	1.49		
1.56				75			1.38		15
1.37		85	90	(136)	90	(126)	1.29		
1.07		120	125	(176)	115	(151)	1.09		
.93				145			1.04		90
.76	85	200	170	(200)	160	(209)	.90	165	
.46	225	295	265	(225)	275	(243)	.70	295	
.33				245			.50	365	
.15	365	365	365		365	(262)	.30		
100 kW full corridor 1/8 door									
2.29				(92)		(76)			
1.98		60		(123)		(116)	1.73		0
1.68		105	55	(156)	50	(155)	1.49		
1.56				95		215	1.38		5
1.37		120	115	(193)	145	(214)	1.29		
1.07		240	185	(240)	230	(284)	1.09		
.93		220					1.04		135
.76	5	415	290	(290)	345	(334)	.90	465	
.46	15	465	465	(338)	465	(374)	.70		
.33				225			.50		
.15	470						.30		

ramp fire full corridor and lobby									
Z meter	T_A	T_C	T_D	P_D (V_D)	T_E	P_E (V_E)	Z meter	T_B	P_B
2.29				(96)		(130)			
1.98				(108)		(184)	1.73		120
1.68		250	190	(120)	280	(210)	1.49		
1.56				220		335	1.38		170
1.37	130	280		(171)	310	(221)	1.29		
1.07	145	335	315	(298)	325	(227)	1.09	335	
.93				340		340	1.04		260
.76	475	690	595	(360)	340	(261)	.90	510	
.46	590	720	720		475		.70	720	
.33				350		345	.50		
.15	720				720	(281)	.30		
100 kW full corridor 1/4 door									
2.29				(100)		(104)			
1.98		70		(116)		(129)	1.73		30
1.68		95	65	(126)	65	(156)	1.49		
1.56				35		150	1.38		35
1.37		120	120	(169)	125	(212)	1.29		
1.07		205	175	(239)		(251)	1.09		
.93				170	195	220	1.04		180
.76	60	340	265	(299)	270	(264)	.90	430	
.46	190	440	410	(342)	410	(324)	.70	440	
.33				175		325	.50		
.15	430		440	(310)	440		.30		

upper surfaces of the burn room. Later, when the surfaces of the adjacent spaces become available for cooling, these losses reach a very large fraction of Q, λ_c approaching the general range .80-.95. These results are consistant with observations in [9].

The Pressure Differential Across the Doorway

For each test run, smoothed data for the time-varying, near-ceiling, pressure differential, Δp, between the burn room and the corridor are presented in Table 2. Δp results are also plotted in Figures 4a and b.

SUMMARY

An experimental program involving a series of dynamic, full-scale, multiroom fire scenarios was carried out. The test parameters included 2 to 3 rooms, 4 different total floor plan areas, 4 different fire energy release rates and 4 widths of doorway between the burn room and the adjacent corridor space. In all, 19 different test runs were carried out.

For all tests, data was acquired from vertical thermocouple and photometer arrays and from video tape records of micro-miniature light arrays.

Taken together the data revealed that intraspace environments in the different rooms of a test configuration could be reasonably described by a two-layer model. Visually, the interface separating the two layers remained relatively sharp until the upper layer grew in thickness to 1/2-2/3 of the room height. Vertical temperature profiles revealed a more diffuse interface. A rule for determining the interface elevation from the vertical instrument array data was formulated and applied to the data of all test runs. The results of this were tabulated in Table 1. A qualified degree of support was seen to be provided for the notion that upper layer filling rates in freely connected multiroom spaces can be estimated from single room model simulations.

For all test runs it was found that the histories of the vertically averaged temperatures at the locations of the 2 or 3 corridor thermocouple arrays were essentially identical. This indicated a certain degree uniformity in conditions along the length of the corridor.

Estimates of the spatially averaged temperatures in each room and for all test runs were obtained and tabulated in Table 2.

The time-varying pressure differential between the burn room and corridor were measured near the ceiling and recorded in Table 2.

A method of estimating the instantaneous total heat transfer out of the bounding surfaces of the test space was formulated and applied to the thermocouple data. The method makes use of rates of change in time of the spatially averaged test space temperature. It estimates the heat transfer as a fraction, $\lambda_c(t)$, of the fire's instantaneous total energy release rate. The histories of the λ_c's which were so estimated are tabulated in Table 2. They indicate that λ_c varied at least within a range .50-.95, where quasi-steady values during the latter times of the test runs typi-

Table 2. Histories of vertically averaged temperatues in burn room, $\overline{\Delta T_A}$, corridor, $\overline{\Delta T_D}$, and lobby, $\overline{\Delta T_E}$; fraction of Q transferred to surfaces, λ_c; near-ceiling pressure drop across doorway, Δp.

25 kW	1/2 corridor				3/4 corridor				full corridor				corridor and lobby				
t sec	$\overline{\Delta T}_C^A$ °C	$\overline{\Delta T}_C^D$ °C	λ_c	Δp torr X10^2	$\overline{\Delta T}_C^A$ °C	$\overline{\Delta T}_C^D$ °C	λ_c	Δp torr X10^2	$\overline{\Delta T}_C^A$ °C	$\overline{\Delta T}_C^D$ °C	λ_c	Δp torr X10^2	$\overline{\Delta T}_C^A$ °C	$\overline{\Delta T}_C^D$ °C	$\overline{\Delta T}_C^E$ °C	λ_c	Δp torr X10^2
10	1.7	0.0		.21	5.1	0.0		.36	0.2	0.0		.09					
20	4.7	0.1		.36	7.9	0.0		.51	1.1	0.0		.09	4.3	0.3	0.0		.44
30	7.0	0.0	.27	.44	10.0	0.0	.44	.67	3.5	0.0	.56	.30	6.1	0.1	0.0	.75	.39
40	8.8	0.1	.34	.48	12.1	0.4	.52	.63	5.6	0.0	.45	.35	6.9	0.2	0.0	.75	.49
50	9.8	0.5	.42	.49	11.7	0.8	.63	.62	6.4	0.0	.47	.52	8.0	0.5	0.0	.72	.54
60	10.9	0.9	.53	.53	12.8	0.9	.66	.58	9.7	0.1	.51	.59	9.8	0.8	0.0	.62	.64
70	12.1	1.2	.61	.48	12.2	1.5	.69	.58	11.2	0.6	.52	.63	10.3	1.0	0.0	.62	.68
80	12.8	2.0	.66	.48	12.4	2.3	.78	.54	12.5	0.9	.60	.68	11.5	1.1	0.0	.70	.66
90	12.9	2.7	.68	.48	13.1	2.8	.75	.54	13.1	1.3	.72	.66	13.5	1.8	0.1	.71	.68
100	13.1	3.2	.66	.47	13.5	3.3	.72	.55	14.3	1.5	.71	.67	12.6	2.4	0.2	.72	.67
110	13.8	3.6	.69	.45	13.2	3.6	.72	.56	14.4	2.2	.73	.68	13.4	2.5	0.0	.83	.59
120	13.6	4.0	.70	.41	13.6	3.6	.70	.51	14.4	2.6	.76	.67	13.1	2.8	0.2	.81	.60
140	14.1	5.0	.74	.41	14.6	4.4	.70	.50	14.4	3.1	.71	.60	13.8	3.2	0.3	.81	.63
160	15.2	5.6	.79	.39	13.4	5.1	.77	.55	14.3	3.4	.78	.57	14.5	3.6	0.6	.78	.64
180	15.7	6.2	.82	.43	15.9	5.6	.80	.54	13.5	3.7	.88	.54	14.2	4.1	0.9	.86	.61
200	15.2	6.6	.83	.42	16.0	6.0	.86	.54	13.8	4.2	.82	.54	15.0	4.5	1.1	.90	.57
300	17.4	7.9	.99	.39	17.2	7.2	.93	.54	15.6	5.2	.93	.57	15.9	5.2	1.6	.96	.66
400	18.1	9.0		.40	16.9	7.8		.51	17.2	6.4	.90	.54	16.1	5.6	2.1	.89	.45
500									17.3	7.0	.92	.55	16.8	6.0	2.2	.97	.46
600									18.8	7.7		.57					
100 kW																	
10	10.2	0.2		.97	5.8	0.0		.57	9.8	0.0		.84	5.9	0.0	0.0		
15	14.8	0.0		1.22	10.4	0.0		.92	17.6	0.0		.99	7.8	0.0	0.0		
20	21.1	0.1		1.34	17.3	0.0		1.11	21.0	0.0	.49	1.32	9.5	0.1	0.0	.74	.66
25	25.5	0.7		1.33	21.6	0.1		1.30	24.1	0.5	.50	1.27	11.4	0.0	0.1	.73	.76
30	26.8	1.4	.38	1.36	24.1	0.8	.44	1.30	27.8	1.2	.54	1.32	15.2	0.3	0.1	.72	.84
35	29.3	2.1	.41	1.47	27.3	1.2	.45	1.45	29.2	2.2	.56	1.34	17.2	0.8	0.0	.71	.97
40	33.3	3.4	.47	1.30	31.2	1.9	.52	1.46	32.8	2.7	.57	1.42	20.7	1.3	0.0	.67	.95
45	34.3	5.2	.46	1.34	30.8	2.7	.55	1.39	34.4	3.2	.55	1.39	23.0	1.7	0.0	.66	1.06
50	35.1	7.0	.51	1.32	33.2	3.3	.54	1.37	34.0	3.9	.60	1.39	25.9	2.1	0.0	.67	1.14
55	35.6	8.2	.53	1.34	34.4	4.1	.58	1.34	35.3	5.0	.60	1.42	28.5	2.8	0.0	.68	1.25
60	36.2	9.5	.63	1.28	34.0	5.8	.64	1.32	35.1	6.2	.60	1.41	29.0	3.7	0.1	.70	1.31
70	37.1	12.2	.65	1.16	35.8	8.4	.67	1.27	36.5	7.6	.64	1.24	33.4	5.3	0.2	.74	1.33
80	40.3	14.5	.63	1.12	36.8	10.4	.67	1.23	37.6	8.4	.67	1.18	34.7	6.6	0.3	.77	1.35
90	41.4	16.7	.69	1.15	36.5	12.2	.67	1.17	41.0	10.6	.69	1.15	36.2	7.6	0.7	.78	1.41
100	42.5	18.6	.73	1.15	39.1	13.7	.66	1.12	39.6	11.4	.75	1.13	37.0	8.1	1.0	.81	1.37
150	50.6	24.0	.80	1.11	48.3	19.0	.82	1.15	45.7	16.8	.79	1.12	39.4	12.2	3.0	.89	1.33
200	55.8	26.5	.89	1.17	52.1	21.9	.90	1.16	49.4	18.8	.90	1.15	43.1	13.8	5.1	.95	1.25
250	56.7	29.2	.93	1.10	54.0	23.7	.89	1.19	53.7	20.5	.93	1.13	45.4	15.4	5.8	.94	1.28
300					55.1	25.6	.94	1.11	54.0	22.1		1.13	44.6	16.4	6.9	.94	1.16
350													45.6	17.3	7.9		
225 kW																	
10	7.2	0.0		.79	8.3	0.0		.80	14.8	0.2		1.11	24.1	0.0	0.1		1.40
15	16.4	0.0		1.12	18.4	0.1		1.18	23.9	0.0		1.60	34.4	0.0	0.1		1.78
20	27.2	0.0		1.46	26.2	0.1		1.58	35.5	0.4		1.76	43.3	0.5	0.1	.65	1.91
25	38.0	0.7		1.64	38.8	0.4		1.91	40.4	1.7		2.16	51.0	2.6	0.1	.68	2.03
30	46.5	1.7	.35	1.82	47.3	1.7	.46	2.01	50.9	2.8	.50	2.26	51.0	3.6	0.1	.70	2.11
35	55.6	3.6	.33	1.78	54.0	3.1	.49	2.32	56.6	4.4	.48	2.31	56.8	4.5	0.1	.72	2.03
40	63.1	6.9	.36	1.80	63.8	4.6	.49	2.27	60.2	6.4	.49	2.38	57.6	5.3	0.2	.74	2.20
45	65.4	11.7	.40	1.73	66.6	7.1	.52	2.10	65.4	9.3	.51	2.48	62.2	9.5	0.3	.76	2.22
50	66.7	14.7	.47	1.62	64.4	10.4	.51	2.02	68.6	11.4	.58	2.43	62.0	10.9	0.4	.77	2.18
55	63.6	18.8	.52	1.60	66.3	13.0	.57	2.01	68.8	13.9	.59	2.30	63.8	11.8	0.5	.78	2.09
60	67.0	20.8	.55	1.42	71.7	15.8	.61	2.03	69.0	15.1	.60	2.10	64.8	13.0	0.8	.78	1.98
70	78.6	28.5	.59	1.39	69.4	19.9	.62	1.71	78.7	17.5	.62	2.11	65.5	15.3	1.5	.84	1.91
80	79.9	33.4	.63	1.37	77.8	23.8	.64	1.79	76.0	21.9	.67	1.96	65.9	17.3	2.5	.85	1.83
90	88.3	37.2	.70	1.33	80.3	28.6	.66	1.68	78.0	25.2	.74	1.85	67.5	18.6	3.7	.85	1.74
100	89.4	39.9	.71	1.17	86.2	32.1	.75	1.61	82.4	27.9	.70	1.78	68.3	19.7	4.8	.87	1.65
150	101.8	47.0	.93	1.29	98.5	38.1	.88	1.53	96.2	35.4	.91	1.71	73.1	24.0	9.2	.93	1.60
200	106.4	52.9	.88	1.32	103.0	43.8	.93	1.61	98.4	39.3	.91	1.80	75.0	26.8	11.7	.96	1.61
250	114.0	58.2	.93	1.26	106.3	47.8	.91	1.58	105.2	43.2	.91	1.76	78.1	29.0	13.4	.94	1.58
300	116.9	63.7		1.27	115.4	51.9		1.59	110.7	45.7	.94	1.70	81.2	30.9	14.8	.98	1.57
350									112.8	48.7		1.76	84.6	32.3	16.0		1.59
ramp																	
10	.1	.1		.16	0.4	0.2		.05	1.7	0.1		.28	1.2	0.1	0.0		.12
20	1.9	.2		.22	0.5	0.2		.07	5.9	0.1		.48	2.2	0.0	0.1	.60	.22
30	3.4	.1	.43	.29	1.6	0.1	.50	.12	7.5	0.2		.56	3.2	1.0	0.0	.63	.24
40	5.0	.1	.53	.38	2.0	0.0	.49	.22	9.9	0.6	.37	.61	4.6	0.0	0.1	.67	.29
50	6.9	.3	.54	.42	4.7	0.1	.57	.33	11.5	0.9	.49	.65	4.7	0.1	0.2	.64	.39
60	8.4	.5	.59	.47	6.5	0.2	.60	.35	12.7	1.5	.66	.67	7.3	0.3	0.2	.67	.45
70	10.2	.8	.64	.54	8.6	0.4	.68	.44	13.8	1.8	.66	.66	9.0	0.4	0.1	.63	.56
80	13.1	1.3	.69	.60	9.4	0.5	.71	.45	14.5	2.4	.65	.71	12.2	0.7	0.2	.67	.62
90	14.9	1.8	.67	.66	10.3	0.7	.70	.50	15.5	3.1	.62	.72	13.8	1.0	0.3	.66	.70
100	17.0	3.0	.70	.67	10.9	1.0	.62	.54	16.6	3.6	.62	.74	16.5	1.5	0.2	.67	.80
150	30.2	9.0	.73	.90	23.8	4.6	.63	.98	25.1	6.2	.67	.96	26.7	4.9	0.6	.74	1.00
200	39.7	16.2	.77	.85	36.1	10.6	.62	1.09	38.4	10.8	.66	1.24	37.5	9.8	1.7	.76	1.29
250	55.1	23.4	.83	1.05	51.9	17.5	.63	1.28	49.4	16.2	.73	1.36	47.2	13.7	3.8	.83	1.36
300									64.3	22.2	.72	1.42	58.7	17.2	6.0	.85	1.54
350									73.4	28.1	.83	1.58	63.1	21.4	8.0	.88	1.57
400									82.6	34.4	.80	1.70	73.5	25.3	10.7	.89	1.62
450													86.2	29.6	13.2	.90	1.73
500													94.8	33.5	15.8	.91	1.72
550													102.6	37.6	18.2	.92	1.80
600													112.8	42.4	20.7		1.88

Table 2. Continued

100 kW	full corridor 1/2 door				full corridor 1/4 door				full corridor 1/8 door			
t sec	$\overline{\Delta T}_A$ °C	$\overline{\Delta T}_D$ °C	λ_c	Δp torr X10^2	$\overline{\Delta T}_A$ °C	$\overline{\Delta T}_D$ °C	λ_c	Δp torr X10^2	$\overline{\Delta T}_A$ °C	$\overline{\Delta T}_D$ °C	λ_c	Δp torr X10^2
10	6.1	0.0		.47	13.8	0.1		1.08	38.3	0.3		2.26
15	6.9	0.0		.73	22.1	0.1		1.49	43.9	0.6		2.34
20	12.1	0.1		.90	29.3	0.2		1.80	48.1	0.7		2.35
25	16.7	0.0	.47	1.18	34.8	0.2	.35	2.03	52.6	0.8		2.45
30	22.7	0.0	.50	1.32	42.1	0.7	.43	2.14	53.7	1.0	.56	2.66
35	26.6	0.6	.50	1.57	45.8	1.0	.49	2.26	59.2	1.1	.61	2.63
40	31.8	1.0	.50	1.70	49.9	1.4	.56	2.30	62.0	1.2	.64	2.77
50	40.3	1.7	.51	1.83	53.4	1.9	.65	2.34	63.7	1.4	.67	2.65
60	43.2	2.5	.58	1.90	57.3	2.1	.66	2.42	70.7	2.2	.74	2.83
70	47.1	5.1	.63	1.98	59.1	3.3	.72	2.47	73.3	2.5	.75	2.76
80	50.2	7.1	.65	1.84	62.4	4.5	.72	2.45	74.4	2.9	.82	2.78
90	49.2	7.0	.67	1.71	68.0	5.1	.72	2.43	76.4	3.6	.84	2.85
100	50.4	8.8	.75	1.75	65.9	5.6	.78	2.39	77.2	3.9	.84	2.94
150	55.7	13.2	.81	1.62	69.0	9.0	.88	2.27	82.6	5.9	.91	2.77
200	57.5	16.5	.88	1.56	72.5	11.2	.90	2.36	87.8	7.0	.90	2.96
250	60.5	18.7	.87	1.67	75.4	12.8	.92	2.29	89.8	8.6	.91	3.08
300	62.7	20.2	.89	1.63	79.6	13.9	.94	2.31	93.9	9.6	.95	2.97
350	64.5	21.7		1.60	79.2	15.1	.90	2.33	96.0	10.4	.95	2.91
400					82.0	15.8	.94	2.40	99.2	11.6	.93	2.87
450									99.6	12.2		3.09

cally fell in the range .80-.95. By these results a major challenge to analysts of enclosure fire phenomena was thereby identified; namely, to provide reasonably accurate apriori estimates for the heat transfer to enclosure boundaries. In this regard, considerable progress in estimating heat transfer to ceiling surfaces of rooms of fire origin has already been made [13,14]. Further advances will require additional results from both experimental and theoretical efforts.

REFERENCES

1 Zukoski, E.E., Development of a Stratified Ceiling Layer in the Early Stages of a Closed-Room Fire, Fire and Materials, Vol. 2, No. 2, pp. 54-22 (1978).

2 Waterman, T.E., and Pape, R., A Study of the Development of Room Fires, IIT Research Institute, NBS-GCR-77-110, prepared for U.S. Department of Commerce, NBS (1976).

3 Emmons, H.W., Mitler, H.E., and Trefethen, L.N., Computer Fire Code III, Harvard Univ. Div. of Appl. Sciences, Home Fire Project Tech. Rept. No. 25 (1978).

4 Zukoski, E.E., and Kubota, T., A Computer Model for Fluid Dynamic Aspects of a Transient Fire in a Two Room Structure (Second Edition), Cal. Inst. Tech. Rept., prepared for U.S. Department of Commerce, NBS (1978).

5 Tanaka, T., A Model of Fire Spread in Small Scale Buildings, Third Joint Meeting U.S.-Japan Panel on Fire Research and Safety, UJNR, Washington, D.C., (1978).

6 Emmons, H.W., The Home Fire Project, Harvard University and Factory Mutual Research Corp. Progress Report, NBS Grant 7-9011 (1980).

7 Tanaka, T., A Model on Fire Spread in Small Scale Buildings - 2nd Report, BRI Research Paper No 84, Ministry of Construction, Japan (1980).

8 Mulholland, G., et al, Smoke filling in an enclosure, 20th Nat'l Heat Transfer Conf., Milwaukee (1981).

9 Cooper, L.Y., Estimating Safe Available Egress Time from Fires, National Bureau of Standards NBSIR 80-2172 (1981).

10 McCaffrey, B., Measurements of the Radiative Power Output of Some Buoyant Diffusion Flames, in preparation.

11 Bukowski, R.W., Smoke Measurements in Large Small Scale Fire Testing, National Bureau of Standards, NBSIR 78-1502 (1978).

12 Steckler, K., Quintiere, J., and Rinkinen, W., Fire Induced Flows Through Room Openings-Flow Coefficients, to appear as National Bureau of Standards NBSIR.

13 Cooper, L.Y., Heat Transfer from a Buoyant Plume to an Unconfined Ceiling, 20th Nat'l Heat Transfer Conf., Milwaukee (1981).

14 Cooper, L.Y., Convective Heat Transfer to Ceilings Above Enclosure Fires, in preparation.

APPENDIX: ESTIMATING THE RATE OF HEAT TRANSFER TO THE ENCLOSURE SURFACES

The energy and continuity equations for the enclosure can be written as

$$\frac{d}{dt}\int_\tau \rho e\, d\tau + \int_S \rho e \bar{V}\cdot\bar{n}\, dS = Q(1-\lambda_c) - P\int_S \bar{V}\cdot\bar{n}\, dS \qquad (A\text{-}1)$$

$$\frac{d}{dt}\int_\tau \rho\, d\tau + \int_S \rho \bar{V}\cdot\bar{n}\, dS = 0 \qquad (A\text{-}2)$$

where ρ is the density, e is internal energy, τ and S are the volume and bounding surface of the enclosure space, and where P, the absolute pressure, is approximated as being uniform in τ. Also, $\bar{V}$ is the velocity and $\bar{n}$ is the outward surface normal vector.

e is now expressed as

$$e = h_{amb} + (h-h_{amb}) - \frac{P}{\rho} = h_{amb} + C_p\,(T-T_{amb}) - \frac{P}{\rho} \qquad (A\text{-}3)$$

where h, the enthalpy, is decomposed into its ambient value, h_{amb}, and variations from h_{amb}. Substituting Eq. (A-3) into Eq. (A-1) and using Eq. (A-2) results in

$$\frac{d}{dt}\int_\tau \rho C_p\,(T-T_{amb})\,d\tau - \tau\frac{dP}{dt} + \int_S \rho C_p\,(T-T_{amb})\bar{V}\cdot\bar{n}\, dS = Q(1-\lambda_c) \qquad (A\text{-}4)$$

The $\tau dP/dt$ term in the above is related to work done as a result of pressure changes within τ, and it will tend to be negligible compared to the energy transfer term on the right-hand side [1]. The surface integral can also be neglected since, by design, leakage from τ is assumed to occur near the floor of the corridor where $T \approx T_{amb}$. Finally, it is reasonable to approximate ρ in the above by ρ_{amb}. Incorporating all of these approximations leads to the Eq. (4) representation for λ_c.